Seasonal Variability of the Florida Current[1]

Pearn P. Niiler and William S. Richardson

Nova University
Fort Lauderdale, Florida 33314

ABSTRACT

The seasonal variability of the directly measured transport and horizontal currents in the Florida Strait has been determined from 90 transects of the Florida Current at the latitude of Miami, Florida. It is estimated that the seasonal variability accounts for 45% of the total variability in the total transport; the early summertime maximum value of the transport is $33.6 \times 10^6 m^3/sec$, and the early winter low is $25.4 \times 10^6 m^3/sec$. The details of the temperature distribution with depth at the season of maximum and minimum flow also have been determined. The seasonal change in the sea level across the Florida Strait is computed from the geostrophically balanced surface velocity and is found to have an amplitude of 6.5 cm. A much smaller (1.3 cm) corresponding seasonal amplitude in the steric level with respect to the ocean bottom has been observed, and the seasonal changes in the sea level are directly related to the seasonal changes in the dynamically induced pressure on the ocean floor. The seasonal changes of the transport in the Florida Strait penetrate to the ocean bottom. The annual cycle of heat transport also is discussed.

I. *Introduction.* Tidal records, ship-drift reports, and electric potential-difference measurements offer the most extensive data on the variability of the current that flows through the Florida Strait. An excellent review of the efforts to relate these data to the variable flow conditions of the Florida Current has recently been provided by Wunsch et al. (1969). They suggest, along with many previous investigators, that the long-term differences in the sea level at various tide stations are related to the seasonal changes in the surface current in this area; they conclude, simply, that the seasonal variability of the surface Florida Current across the Strait is 10% of the average value. Their analysis incorporates hourly tidal readings that span many years, and the statistical significance of their conclusions on the nature of the sea-level variations is certainly reliable. Sea-level differences, however, are an indirect measure of the flow conditions; no detailed direct measurements of the seasonal cycle in the currents have been reported.

Two other types of surveys have been instrumental in the effort to unravel the magnitude of seasonal fluctuations of the Florida Current. The first of these

1. Accepted for publication and submitted to press 1 May 1973.

is the experiment carried out in 1962–1964 by the University of Miami in an effort to determine the seasonal variability of the hydrographic structure within the Florida Strait. Thirteen consecutive monthly cruises were undertaken and hydrographic stations were made at six equally spaced points across the Strait at the Miami latitude. Broida's (1962–1964) review of these data reveals that as much variability in the hydrographic conditions occurred from one monthly cruise to the next as was apparent in cruises separated by two seasons. The study helped to establish the seasonal cycle of the temperature of near-surface waters, but it did not provide a large enough sample to ascertain this variability in the deeper water.

Records on the electric potential difference between two electrodes represent the second type of study; these records have been maintained since early 1969 at two locations in the Florida Strait. The electric potential difference is a measure of the total transport of seawater flowing over the cable, and the cable-electrode configuration must be calibrated by direct measurements of the transport in order that the data can be related quantitatively to the flow conditions. The University of Miami (de Ferrari, personal communication) has maintained a calibrated electrode pair in the western portion of the Strait, with an eight-mile electrode separation; Sanford (personal communication) of the Woods Hole Oceanographic Institution has maintained a record of the potential difference between Palm Beach, Florida, and Grand Bahama Island. These studies are not yet complete, but they should handsomely complement the three-year record that was obtained by Wertheim (1954) on the telegraph cable between Key West, Florida, and Havana, Cuba. Unfortunately, the present Miami cable does not span the entire channel, and the Palm Beach and Key West cables have not been calibrated.

A twofold problem has persisted in determining the seasonal variability of the Florida Current. When an adequate record length of a variable at a few locations can be obtained (such as tidal heights or cable potential readings), the interpretation in terms of the flow conditions is difficult and usually yields only qualitative information about the three-dimensional structure of the current; the shorter records of more direct measurements, while containing a wealth of information, are so contaminated with short-period fluctuations that they do not shed light on the annual cycle. Though unknown when the University of Miami's thirteen-month survey was started in 1962, it is now a well-established fact that the short-period (less than two weeks) modulation in both the velocity and the hydrographic structure of the Florida Current is as large as the seasonal changes.

This is a report on an experiment to determine the seasonal variabilities in the Florida Current by direct means. Over the years 1964–1971, numerous samples of the horizontal velocity were gathered at a number of depths at identical locations at the Miami latitude; the temperature structure was measured concurrently with the velocity. The seasonal changes determined from these data give an adequate picture of the variability of the two-dimensional cross-stream structure. The aliasing problem is dealt with in the following pragmatic manner.

A seasonal average of a measurement is determined from an appropriately calculated average of a number of random samples that were gathered during a two- or three-month period (in a number of different years). It has been possible to show that when more than ten samples of, for example, the transport of the Florida Current are used to form such an average, no significantly different average (no change in an r.m.s. fit or in the error of the mean) is obtained from ten different samples that belong to the same period or to the same period in a different year. Effectively, a low-pass filter is applied to the data, without determining the phase or amplitude of the short-period fluctuations explicitly. The standard error of the mean for a particular season is estimated on the basis that the shorter-period fluctuations are white noise. This method is analogous to that devised by Thompson (1971) to analyze the long-period fluctuations in gappy current-meter records at Site D in the North Atlantic, and statistical credence, if not certitude, is obtained for the variability that is interpreted as seasonal changes. It is clear that a more definitive study, one that could increase the statistical reliability of the data by a factor of two, would require a fourfold effort compared with that already expended.

II. *The Experimental Method and the Scope of the Data.* The data on the density and velocity structure of the Florida Current that are presented and discussed here have been gathered by the free-drop method. The method for obtaining measurements of the vertically averaged horizontal velocity and the accuracy of the data-acquisition system have been discussed by Richardson and Schmitz (1965). The temperature structure was obtained from a freely falling STD. The temperature sensor of the STD (Bissett-Berman Corp., Model 9060) has proved to be reliable, but the reliability of the conductivity system used to determine the salinity is questionable. With no apparent change in the calibration of the conductivity cell, values of salinity below 400 m were occasionally lower than the historical salinity data for this region by as much as $0.6^0/_{00}$. Because of this difficulty, the seasonal picture of the density structure has been based on the local seasonally averaged historical temperature-density correlation rather than on direct measurements. The specific method used to form a seasonal average, together with estimates of its statistical reliability, is outlined during the subsequent presentation of the variabilities in the transport, the horizontal-velocity distribution, and the temperature and density structure.

For convenience, each excursion of the ship from port is termed a "cruise." During a normal cruise of eight hours, the surface current, the average horizontal velocity to a number of depths, and a record of the temperature versus depth were obtained at 13 closely spaced stations along the transect from Miami to Bimini. The location of the stations and the transect in the Florida Strait

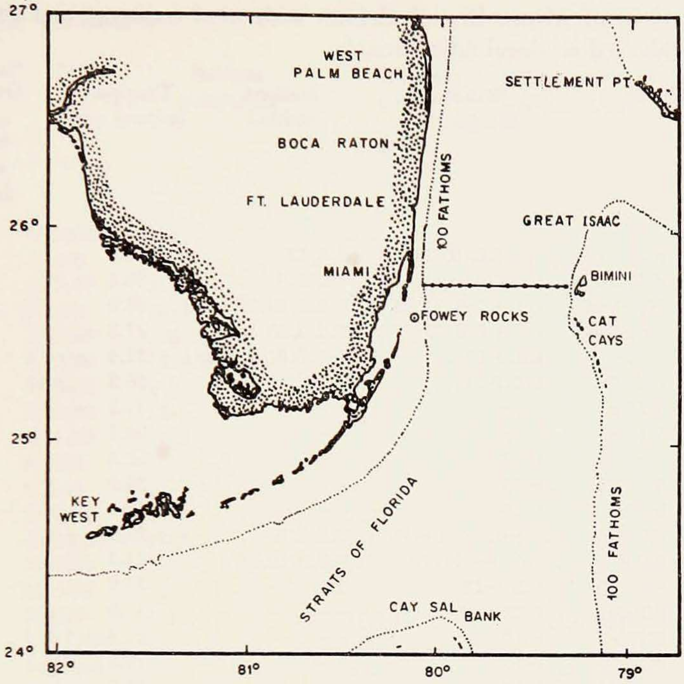

Figure 1. Station locations.

are shown in Fig. 1. The record of this experiment is tabulated in Table I. A total of 3682 dropsonde records and 336 STD records make up the bulk of the data.

Some of these data have been used by various investigators in describing and discussing the average dynamic and kinematic structure of the Florida Current (Richardson and Schmitz 1968, Richardson et al. 1969, Schmitz 1969, Schmitz and Niiler 1969, Broida 1969, Wunsch et al. 1969, Stubbs 1971, Duing and Johnson 1972, de Ferrari, personal communication). This is the first presentation of a comprehensive study of the entire archive in terms of the seasonal patterns. The National Oceanographic Data Center maintains a file of the dropsonde data, and Nova University has a file of the STD temperature records.

III. *The Seasonal Variability*. A. The Transport. The transport of the Florida Current, tabulated in Table I, was computed by a cross-channel numerical integration of the observations of the northward component of transport per unit width during each individual cruise. The maximum value of the 75 samples is $38.2 \times 10^6 m^3 sec^{-1}$, in the summer of 1965; the minimum value is $19.0 \times 10^6 m^3 sec^{-1}$, in the winter of 1970. Not all of this variability

Table I. List of Miami-Bimini Cruises with total transport and geostrophically balanced sea-level difference.

Sequential* cruise number	Date	Stations completed	Stations omitted	Transport (m^3/sec) × 10^6	Geostrophically balanced sea-level difference (cm)
1	8/16/64	1,2,4,6–10,13	3,5,12	36.0	--
2	8/17/64	12,9–5,3–1	13,11,4	36.8	--
3	10/20/64	1,2,5,7–9,11,13	3,4,6,10,12	33.0	--
4	10/22/64	1,2,4,6–8,12,13	3,5,9,10,11	27.2	--
5	12/14/64	4,6,7,10,11	1–3,5,8,9,12,13	32.4	--
6	4/5/65	1–8,10,11,13	9,12	36.3	68.5
7	5/24/65	1–13	--	31.2	80.8
8	5/26/65	1–13	--	34.1	76.3
9	5/28/65	1–13	--	38.2	86.7
10	5/30/65	1–13	--	34.9	72.1
11	6/4/65	1–13	--	29.2	56.0
12	6/6/65	1,3,4,7–9,11–13	2,5,6,10	26.9	65.8
13	6/8/65	1–3,5–7,11,12	4,8,9,10,13	31.7	68.0
14	6/12/65	1,3,4–13	2	35.0	83.6
15	6/16/65	1–13	--	37.9	72.3
16	6/18/65	1–13	--	31.4	69.5
17	6/21/65	1–13	--	29.2	65.9
18	6/23/65	1–13	--	33.0	70.7
19	3/24/66	1,3,6–8,10,13	2,4,5,9,11,12	32.4	--
20	5/28/66	1,3,5–8,13	2,4,12	30.1	--
21	12/4/66	1,7–13	2–6	32.8	--
22	11/15/67	1–13	--	28.5	42.1
23	11/16/67	13–8,6	9,5–1	N.G.	--
24	12/7/67	1–13	--	22.0	58.7
25	12/8/67	13–1	--	26.5	63.3
26	1/3/68	1–13	--	24.4	63.1
27	1/4/68	13–1	--	26.5	68.2
28	2/10/68	1–13	--	24.3	45.0
29	2/12/68	13–1	--	26.5	58.5
30	3/30/68	1–13	--	35.3	67.8
31	3/31/68	13–1	--	35.2	81.3
32	4/4/68	1–13	--	33.2	82.8
33	4/5/68	13–1	--	33.8	86.2
34	4/10/68	1–13	--	32.4	86.2
35	4/11/68	13–1	--	31.7	76.8
36	4/17/68	1–13	--	33.2	74.0
37	4/23/68	1–13	--	28.2	68.5
38	4/24/68	13–1	--	25.6	62.3
39	4/26/68	1–13	--	32.5	61.4
40	4/27/68	12,10,8,6,4,2	13,11,9,7,5,3,1	34.0	71.5

* Cruises missing in the sequential list were carried out, but no usable data were obtained.

Table I – continued.

Sequential* cruise number	Date	Stations completed	Stations omitted	Transport (m^3/sec) × 10^6	Geostrophically balanced sea-level difference (cm)
41	4/30/68	1–13	– –	32.3	64.5
42	5/1/68	13–1	– –	31.4	60.7
43	4/29/69	2–10	1, 11, 12, 13	28.9	61.5
44	5/1/69	1–13	– –	35.5	71.3
45	5/27/69	1–8, 10, 11	9, 12, 13	31.8	70.5
46	5/28/69	13–9, 7, 6, 5, 3, 2	1, 4, 8	29.5	76.7
47	5/29/69	1–8, 10–13	9	34.1	70.2
48	5/30/69	12–1	13	33.2	66.6
49	5/31/69	1–13	– –	35.8	73.3
50	6/1/69	12–5, 3–1	4, 13	29.2	64.4
52	6/3/69	13–9, 7–1	8	33.5	70.3
55	11/2/69	1–13	– –	25.4	37.4
56	11/13/69	13–3	2, 1	27.0	46.3
57	11/4/69	1–13	– –	26.8	42.9
58	11/5/69	13–1	– –	23.9	34.5
59	11/8/69	1–11	12, 13	23.4	32.5
61	11/12/69	1–13	– –	20.1	42.1
62	11/13/69	13–1	– –	24.1	48.8
63	12/1/69	1–4	5–13	– –	– –
65	12/15/69	1–13	– –	28.0	50.8
66	12/16/69	13–1	– –	29.8	52.1
67	12/18/69	1–13	– –	28.4	59.9
68	12/19/69	13–9, 6–1	8, 7	N.G.	– –
69	1/13/70	1–10	11–13	26.1	52.3
70	1/14/70	13–1	– –	24.9	52.9
73	1/22/70	1–13	– –	19.0	44.6
74	1/23/70	13–1	– –	19.7	45.2
75	1/27/70	1–13	– –	27.4	59.7
77	2/12/70	1–13	– –	27.4	52.6
78	2/13/70	13–1	– –	26.9	57.0
79	9/9/70	1–13	– –	32.8	72.0
81	9/16/70	1–13	– –	27.4	67.4
82	9/17/70	13–7	6–1	– –	– –
83	9/23/70	1–13	– –	32.6	70.5
84	9/24/70	13–9	8–1	– –	– –
85	10/2/70	1–13	– –	22.2	48.5
86	1/4/70	13–10, 7–1	9, 8	N.G.	– –
87	10/15/70	1–6, 8–13	7	21.4	47.7
88	10/16/70	13–6	5–1	23.3	50.3
89	11/2/70	1–13	– –	20.5	49.0
90	11/3/70	13–1	– –	23.4	56.8

* Cruises missing in the sequential list were carried out, but no usable data were obtained.

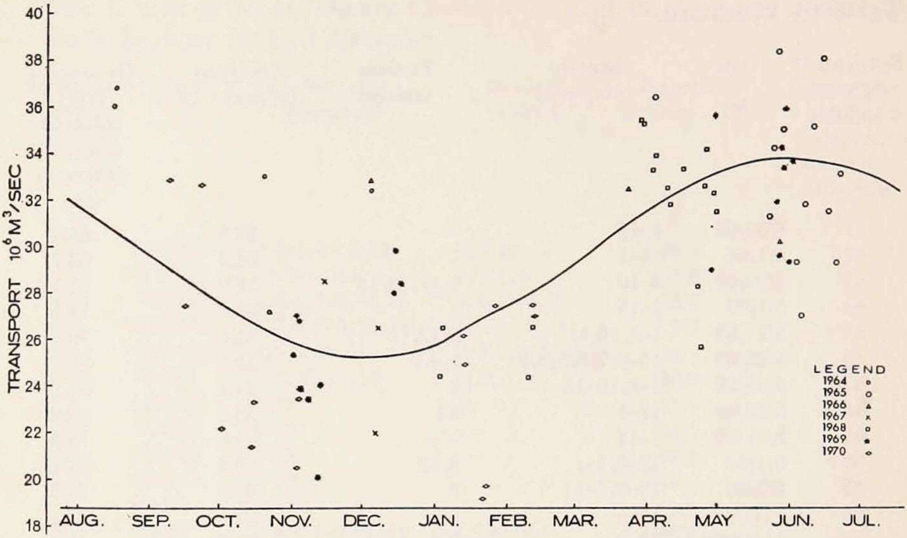

Figure 2. Annual cycle of the total transport of the Florida Current.

is correlated with the changing seasons. The entire set of data is plotted in Fig. 2, from which it is apparent that as much variability occurs within a particular season as from season to season. Three intensively sampled sets of data were gathered in the early summertime of the years 1965, 1968, and 1969; they comprise 12, 13, and 9 cruises, respectively. The seasonal pattern is repeated in these years, the respective summertime averages of the transport being $32.7\ (\pm 3.3)$, $31.0\ (\pm 2.8)$, $32.4\ (\pm 2.5) \times 0.10^6 \mathrm{m}^3 \mathrm{sec}^{-1}$. The term in parentheses is the standard-error estimate of the mean.

The solid line in Fig. 2 is the best fit to the annual harmonic. The mean value of the transport is $29.5 \times 10^6 \mathrm{m}^3 \mathrm{sec}^{-1}$; the annual harmonic, with $\omega_A = 1$ cycle per year, is $A \cos(\omega_A t - \psi)$, having an amplitude $A = 4.1 \times 10^6 \mathrm{m}^3 \mathrm{sec}^{-1}$ and a phase $\psi = 2.7$ radians (22 weeks), measured from 1 January. The maximum transport thus occurs in early June. This curve is not altered significantly if the semiannual, the diurnal, and the semidiurnal tidal terms are included in the harmonic tidal analysis.

The second method for determining the seasonal variability of the transport is to analyze the annual variation of the transport per unit width at each station and then to integrate this function across the current. If $a(x)$ is the amplitude of the annual harmonic at a location $x[L_0 < x < L]$ in the current and if $\varphi(x)$ is the phase, the seasonal harmonic and phase are obtained from:

$$A \cos(\omega_A t - \psi) = \int_{L_0}^{L} a(x) \cos[\omega_A t - \varphi(x)]\, dx.$$

Table II. The annual harmonic transport per unit width in the Florida strait. The origin of the coordinates is at Virginia Key, Miami, Florida.

Station number	Location x (km)	No. of samples	$a(x)$ $m^2 sec^{-1}$	$\psi(x)$ radians
1	10	69	25	1.3
2	15	71	21	1.6
3	20	72	24	2.8
4	25	68	29	2.7
5	30	71	30	2.6
6	35	72	50	3.2
7	45	70	72	2.2
8	55	70	95	2.3
9	65	69	82	2.6
10	70	71	75	2.5
11	75	69	66	2.7
12	80	68	60	3.1
13	83	63	62	3.0

The amplitude and the phase of the annual harmonic of the northward component of transport per unit width at each station are shown in Table II.

The numerical integration of the data in Table II yields $A = 4.0 \times 10^6 m^3 sec^{-1}$ and $\psi = 2.5$ radians, which confirms the result obtained by first integrating the cruise data for the transport and then computing the annual cycle.

We are not aware of any theory that adequately explains the character of the seasonal change of the transport of the Florida Current. The wind-stress curl over the trade-wind zone is at a maximum in the month of February (Hellerman 1965), and the wind-driven transport (the Sverdrup transport) should respond directly, with a short time lag, to this forcing. Veronis and Stommel (1956) have shown that no internal waves of yearly period (on the scale that is imposed by the seasonal cycle of the wind stress) can propagate on the main extra-equatorial thermocline, and they have suggested that the response of the ocean to seasonal forcing should be barotropic. Lighthill (1969) has shown that baroclinic currents near the equator lag the time-history of the wind stress by only a month (not four months, as is observed here). In fact, as predicted by Lighthill, the Indian Ocean circulation and the Somali Current respond quickly to the change in the monsoon pattern (Leetma 1972, Duing 1970). Gill and Niiler (1973) have considered the simplest theory for the seasonal changes in the North Atlantic and Pacific oceans: one that isolates the barotropic response in the basin of variable topography. Their calculation of the amplitude of the barotropic response in the trade-wind currents of the North Atlantic is commensurate with what is the measured response of the Florida Strait; however, the maximum value occurs in phase with the wintertime maximum value of the wind-stress curl. In none of these theories is the role of the western and eastern boundary currents, equatorial currents, and continental shelves or

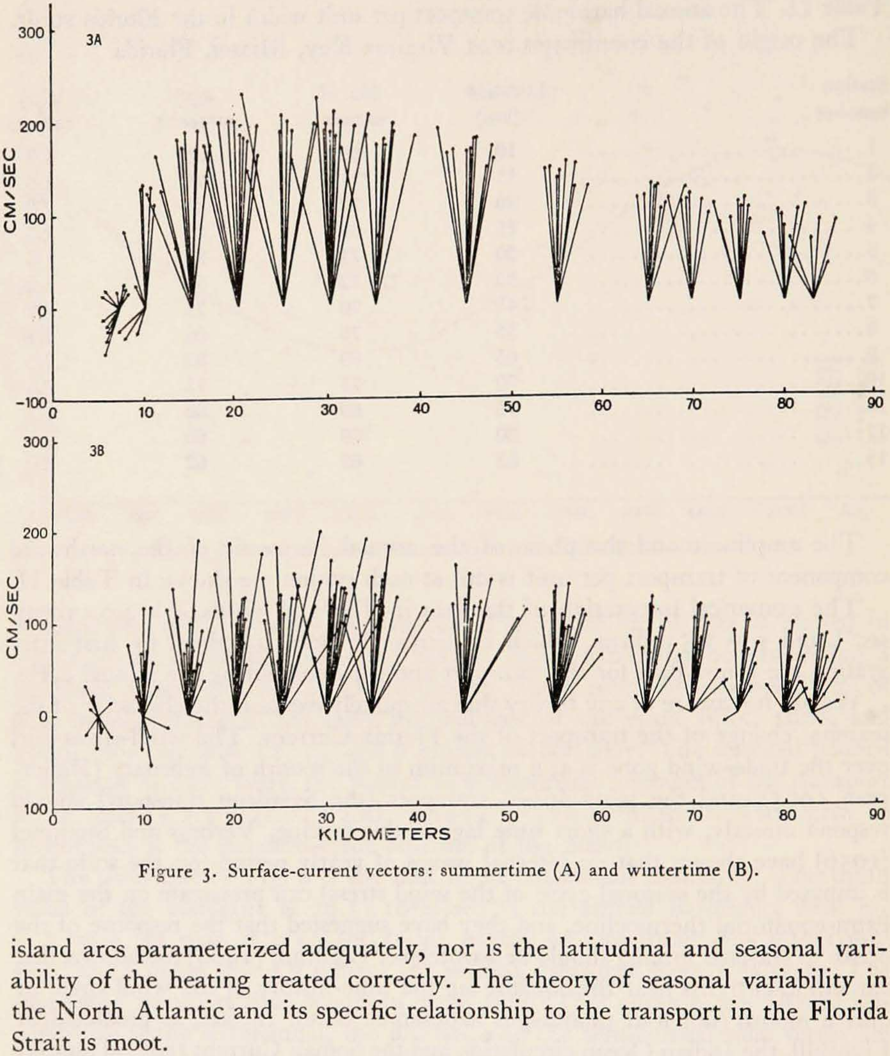

Figure 3. Surface-current vectors: summertime (A) and wintertime (B).

island arcs parameterized adequately, nor is the latitudinal and seasonal variability of the heating treated correctly. The theory of seasonal variability in the North Atlantic and its specific relationship to the transport in the Florida Strait is moot.

B. The Horizontal-velocity Structure. The seasonal contrast in the surface pattern across the Miami-Bimini sections is shown in Fig. 3: in Fig. 3 A, the 1969 early summertime observations of the surface velocity vectors, and in Fig. 3 B, the 1970 wintertime data. The velocity distributions at only the season of maximum and minimum transport are presented, because on monthly charts the shorter time-period variability would obscure the seasonal component. The observed increase in transport is reflected partly in the intense summertime surface flow in the western portion of the channel, which has a

Table III. Harmonic analysis of surface current.

Station number	Mean value of current North (cm/sec)	Mean value of current East (cm/sec)	Annual cycle, Current north: Amplitude (cm/sec)	Annual cycle, Current north: Phase radians	r.m.s variability (total) (cm/sec)	r.m.s variability (harmonics removed)* (cm/sec)
1.......	74.8	−11.8	23.1 ± 9.9	3.6 ± 0.3	65.1	60.5
2.......	99.3	6.3	38.1 ± 8.0	1.2 ± 0.3	66.2	55.4
3.......	137.8	0.3	17.6 ± 9.0	2.5 ± 0.4	53.8	45.4
4.......	151.2	5.7	21.3 ± 8.6	2.7 ± 0.3	48.6	35.5
5.......	163.0	7.5	15.5 ± 5.9	2.4 ± 0.3	36.9	23.6
6.......	161.5	4.9	15.0 ± 6.3	2.5 ± 0.3	31.5	20.2
7.......	150.6	2.6	4.6 ± 6.4	2.2 ± 1.3	27.0	17.9
8.......	123.6	3.3	26.0 ± 4.5	2.2 ± 0.1	26.9	19.0
9.......	98.3	0.0	22.8 ± 3.3	2.0 ± 0.2	25.8	19.3
10.......	94.4	−3.2	15.2 ± 2.6	2.2 ± 0.2	25.9	20.1
11.......	83.7	2.0	9.7 ± 2.7	2.7 ± 0.3	28.3	21.0
12.......	72.0	6.0	15.5 ± 3.1	2.8 ± 0.2	33.3	27.6
13.......	68.7	9.4	22.5 ± 4.0	2.6 ± 0.2	40.8	34.7

* The following harmonic constituents were removed by least-squares analysis: annual, semiannual, and the K_1, O_1, M_2, S_2 tidal terms.

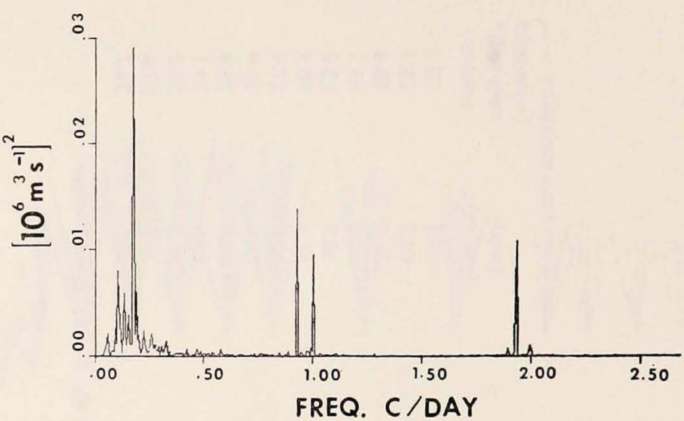

Figure 4. Periodogram of transport variability from electric-potential measurements between Sts. 1 and 3.

maximum value of 190 cm/sec; in the wintertime the maximum flow occurs more to the east, with a maximum speed of only 130 cm/sec.

An estimate of the seasonal variability of the surface current can again be obtained by an harmonic analysis of the entire data set on a station-by-station basis. Table III lists the amplitude and phase of the annual harmonic of the northward component of the surface current for each station. The semi-annual, diurnal, and semidiurnal tidal components are not presented. The estimate of the standard error in Table III is based on the assumption that the r.m.s. of the residual series is created by white noise. Perhaps this error is an overestimation, for the background spectrum is in fact not entirely white.

An example of a measurement capable of quantifying the variability in the frequency band that has not been treated in this harmonic analysis is provided by the two-year record of the calibrated electrode cable located eight miles off Virginia Key. Fig. 4 displays the high-frequency spectrum of the transport fluctuations over this short cable length between St. 1 and St. 3. It is seen that motions with periods between 6 and 14 days are more energetic than the tidal fluctuations, and a considerable part of the r.m.s. of the residual in this analysis is due to these fluctuations and not to white background noise.

The variation of the horizontal velocity with depth has been obtained from the measurement of the vertically averaged current with depth. If $\vec{V}_{av}(z)$ is the vertically averaged velocity to a depth z, then the transport per unit width is $z\vec{V}_{av}(z)$, and the horizontal velocity $\vec{V}(z) = [\partial/\partial z]\,[z\vec{V}_{av}(z)]$. Figs. 5 (A to F) show, respectively, the 1965, 1968, and 1969 summertime data of the transport per unit width as a function of depth at Sts. 3 and 9. Each data point represents a separate observation and indicates the vertical sampling scale normally employed. The solid curve is the least-square quartic fit to the data. Again, it is seen that the seasonal pattern in the northward component of the transport per unit width is reproduced from year to year.

The horizontal-velocity distribution throughout the vertical cross section in the early summer and early winter seasons has been obtained from an r.m.s. polynomial fit to the measurements of the averaged current on a station-by station basis; from this the contours of the isotachs are constructed. Figs. 6 A and 6 B show, respectively, the summer and winter seasonal patterns of the northward flow; Figs. 7 A and 7 B display the summer and winter patterns for the eastward component. In determining the eastward component, it has been found that the mean value is less than the fluctuations, and the error in defining the mean of 10 samples is as large as the mean value itself.

A detailed comparison of the distribution of the northward component of velocity with depth has also been made for three stations. Fig. 8 shows the seasonal contrasts of northward velocity at Sts. 5, 8, and 12 (solid lines for summer, dashed lines for winter). The most remarkable feature of the pattern is apparent at Sts. 8 and 12: the seasonal changes of the northward component of the velocity below the mixed layer (vide next section for discussion of the mixed layer) are independent of depth. This feature will be explored further following presentation of the density structure that is associated with the seasonal pattern of velocity distributions. It will be shown that the seasonal changes in the transport of the Florida Current penetrate to the bottom while the changes in the density field are confined primarily to the upper 100 m of the water column.

C. The Temperature and Density Structure. The most characteristic feature of the seasonal changes in the temperature structure of the subtropical oceans is the formation of the thermocline during the season of summertime heating. Progressively warm layers of water are formed near the surface, and the mixing action of the wind and waves is restricted to a much shallower mixed layer than is present in winter. This pattern is essentially the same in the Florida Current. As can be seen from a typical summertime STD trace at Sts. 4 and 10 [Figs. 9 A, B], a shallow mixed layer overlies warm surface water (>28°C), and the bottom temperature at the shallower station under the Current axis is near 6°C. The wintertime pattern, also shown in Fig. 9, can be identified by the presence of a deeper and colder mixed layer on the surface above the somewhat warmer subsurface waters. At St. 10, the column of relatively homogeneous water between 17°C and 18°C marks an intermediate minimum of the temperature gradient. Worthington (1959) has discussed the horizontal distribution of this peculiar feature of the North Atlantic temperature structure and has shown that in the wintertime this feature is found as far south as 20°N. In the winter, this feature is apparently advected into the

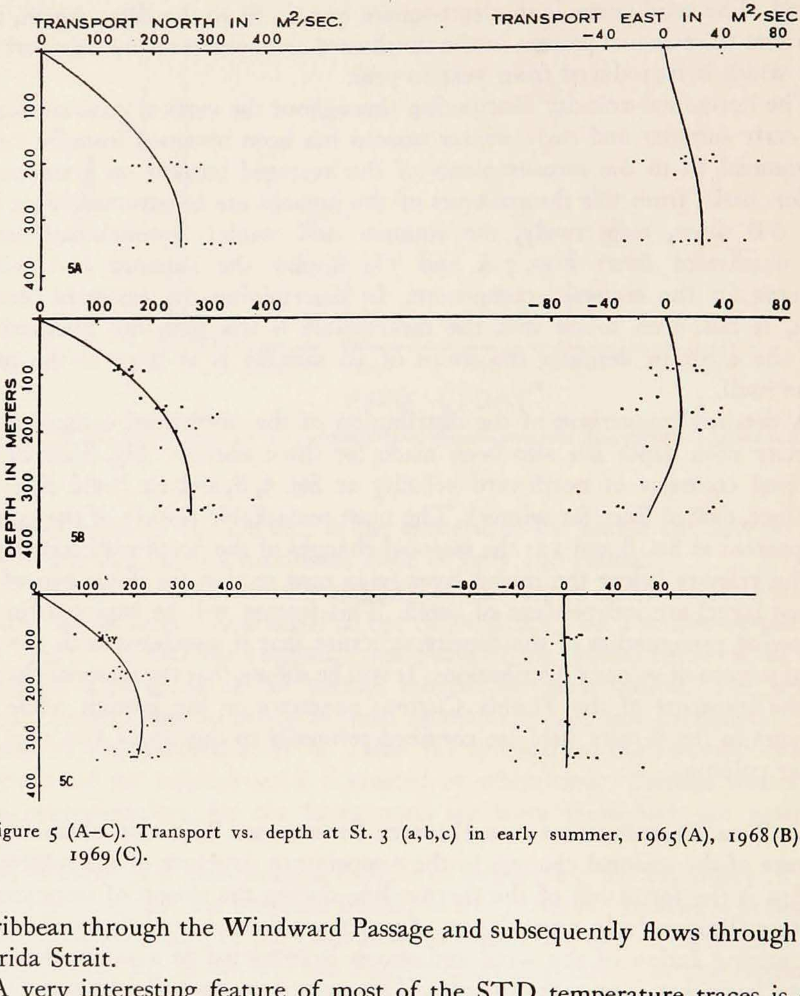

Figure 5 (A–C). Transport vs. depth at St. 3 (a, b, c) in early summer, 1965 (A), 1968 (B) and 1969 (C).

Caribbean through the Windward Passage and subsequently flows through the Florida Strait.

A very interesting feature of most of the STD temperature traces is also apparent in these figures. On a large number of occasions, in both summer and winter, a mixed layer appears along the ocean bottom as well. This layer is found randomly at all the stations, though seldom at Sts. 1, 5, and 13; presumably it is caused by the strong mixing action of the vertical shear along the rough bottom topography.

The two-dimensional structure of the temperature field below the mixed layer is displayed in Fig. 10; this figure was constructed by first reading the temperature at every 25-m interval from the STD records, after which the seasonal arithmetic average temperature and standard deviation were computed at each level. The depth of each isotherm then was graphically determined and the isotherms were contoured.

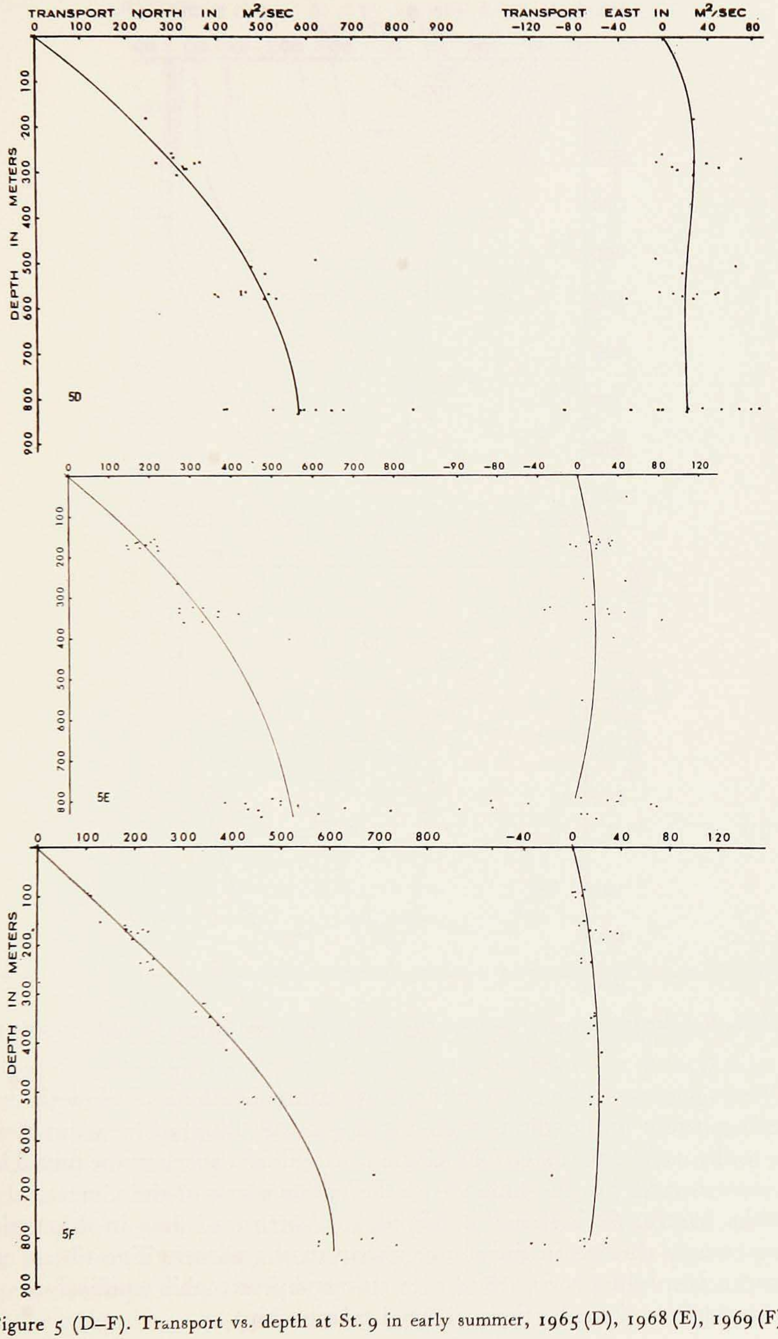

Figure 5 (D–F). Transport vs. depth at St. 9 in early summer, 1965 (D), 1968 (E), 1969 (F).

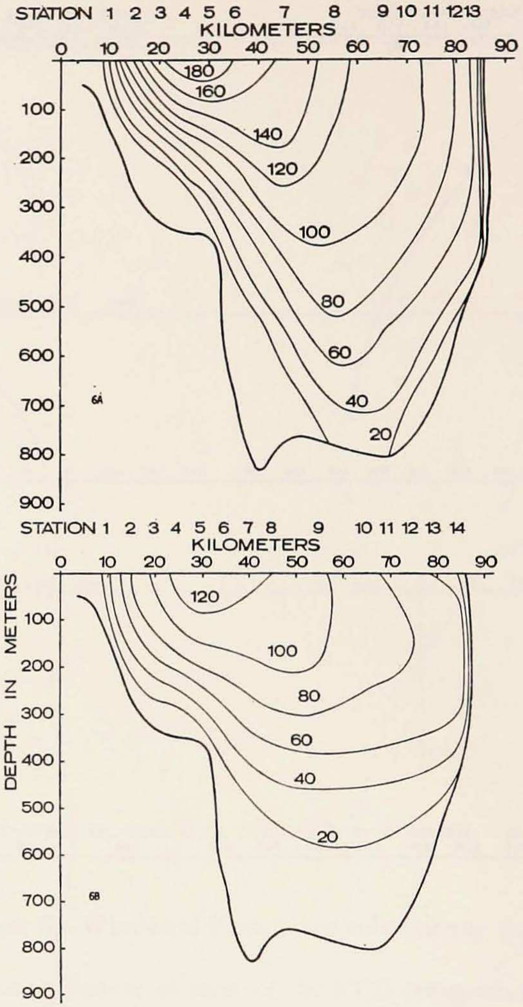

Figure 6. Velocity structure (northward component, cm/sec): summertime (A) and wintertime (B).

The largest seasonal change in the temperature distribution below the mixed layer is apparent in the summertime tilting (or upwelling) of the main thermocline to the west of the axis of the Current. At all depths below the mixed layer, the wate is colder in the summer on the cyclonic side of the Current than it is in the winter. As is shown in Fig. 8, the northward flow in this region is more strongly sheared in the summer than in the winter. The tilting of the isotherms is consistent with the hydrostatic and geostrophic equilibrium of the northward flow (i.e., the thermal wind relationship).

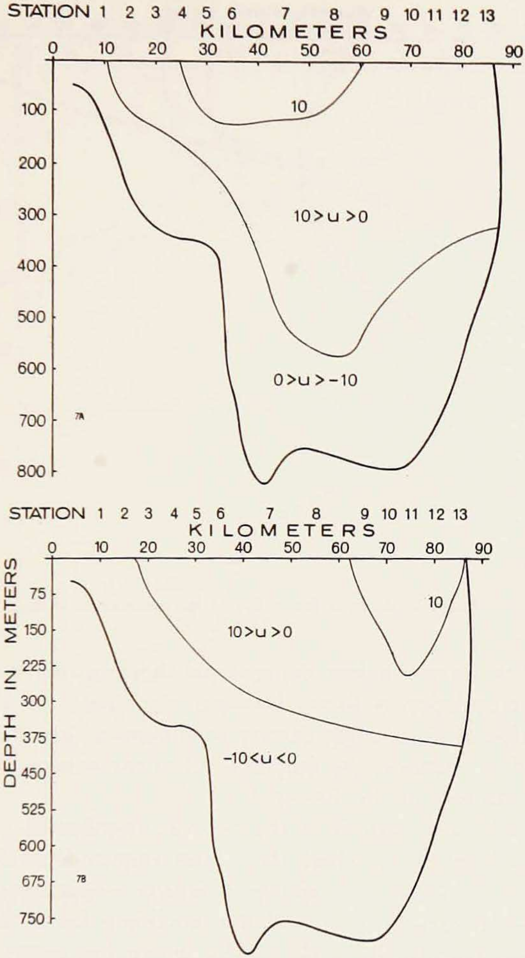

Figure 7. Velocity structure (eastward component, cm/sec): summertime (A) and wintertime (B).

Since the salinity sensors proved to be unreliable in the particular STD that was used for this experiment, the density structure has been derived from an historically established temperature-density correlation of the water mass in the Strait. The hydrographic measurements from the University of Miami's 13-month survey were employed to determine this correlation. The water mass along the cyclonic side of the Current exhibits the Gulf of Mexico characteristics in the summertime, which also is the time when a well-developed intrusion of the loop current generally occurs in the Gulf (Leipper 1967); in the wintertime, the North Atlantic mid-depth water mass fills nearly the entire channel. Fig. 11 displays the temperature and density correlation that prevails in the

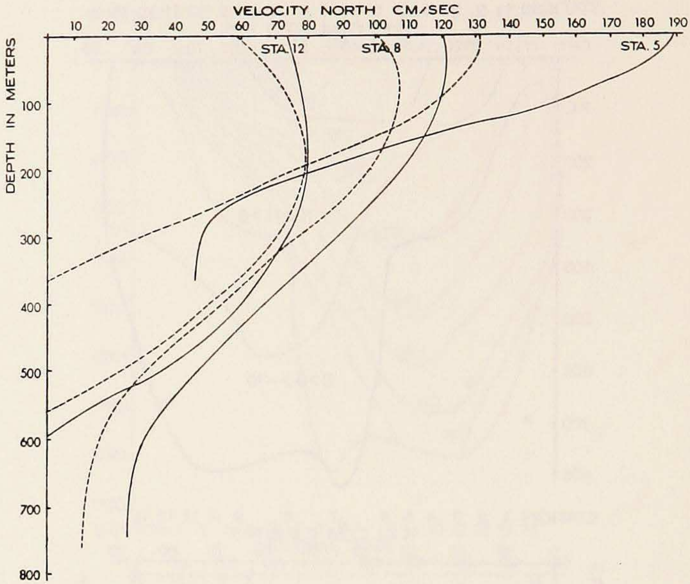

Figure 8. Northward velocity vs. depth at Sts. 5, 8, and 12: summer, solid line; winter, broken line.

western part of the Strait; below the seasonal thermocline, no significant difference in this correlation is found between the seasons in the eastern part.

The distribution of the average density with depth at Sts. 5 and 10 is shown in Fig. 12. At these stations, the deepest level of the seasonal change does not penetrate to the bottom of the Channel.

Fig. 12 displays three regions of the vertical distribution of density. Near the surface is the layer (I) in which the largest amplitude in the seasonal variability of density is apparent; below this seasonal thermocline is found the main thermocline (II), which lies between σ_t 24.5 and 27.0. This body of water is always present between Sts. 2 and 12. Below the main thermocline, (III) the density (and temperature) gradients are an order of magnitude smaller, and the historical data indicate that the water column is of homogeneous salinity ($34.85 > S‰ > 34.78$). The principal seasonal changes in the two-dimensional structure of the horizontal-velocity and density structure is shown in Fig. 13. Table IV gives a summary of the distribution of transport in the three regions. The transport distribution with

Table IV. Seasonal variability of the total-transport distribution in the thermocline. See Fig. 14 for the definition of regions. The values give the flow between Sts. 2 and 12.

Region	Seasonal range ($\times 10^6 m^3 sec^{-1}$)	Mean value ($\times 10^6 m^3 sec^{-1}$)
I	2.7	6.3
II	2.3	18.9
III	2.9	4.1
Total Transport	7.9	29.3

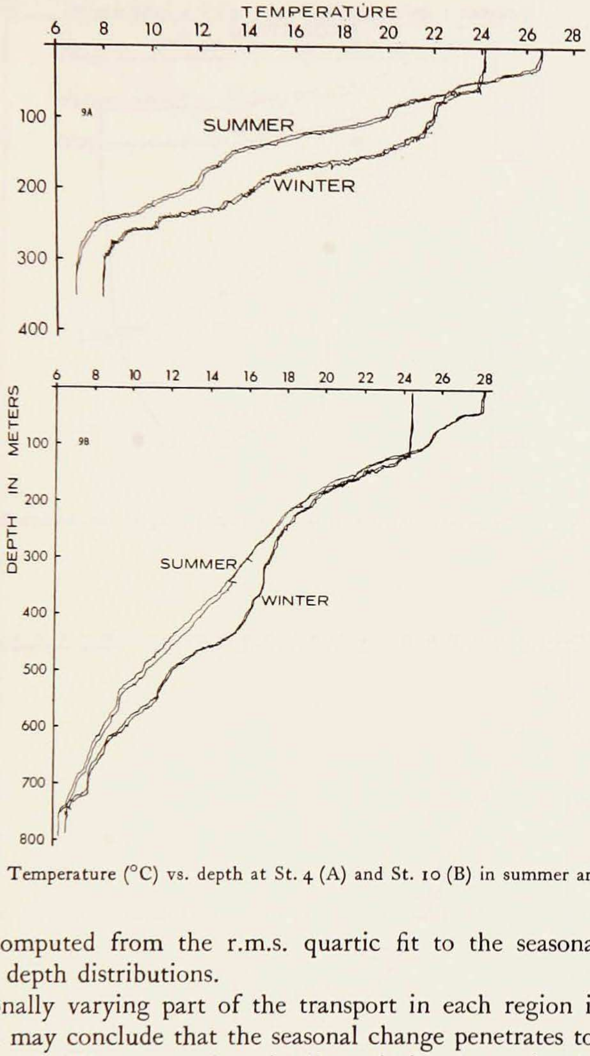

Figure 9. Temperature (°C) vs. depth at St. 4 (A) and St. 10 (B) in summer and winter.

depth was computed from the r.m.s. quartic fit to the seasonally grouped transport vs. depth distributions.

The seasonally varying part of the transport in each region is nearly the same, so one may conclude that the seasonal change penetrates to the bottom of the Channel. The seasonal variability within the main thermocline is smaller, percentagewise, than it is below the thermocline or within the seasonally active layer. The 27.0 σ_t also marks the level below which the water column is of relatively homogeneous salinity. It is apparent that more South Atlantic Intermediate Water participates in the circulation in the summer than in the winter.

D. The Transport of Heat. The transport of heat per unit width through the Channel was computed from

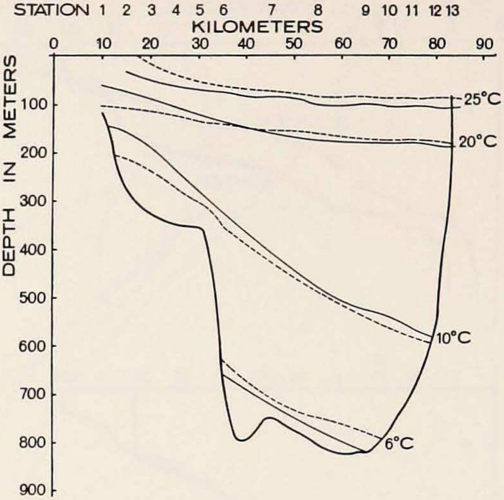

Figure 10. Temperature structure: summer, solid line; winter, broken line.

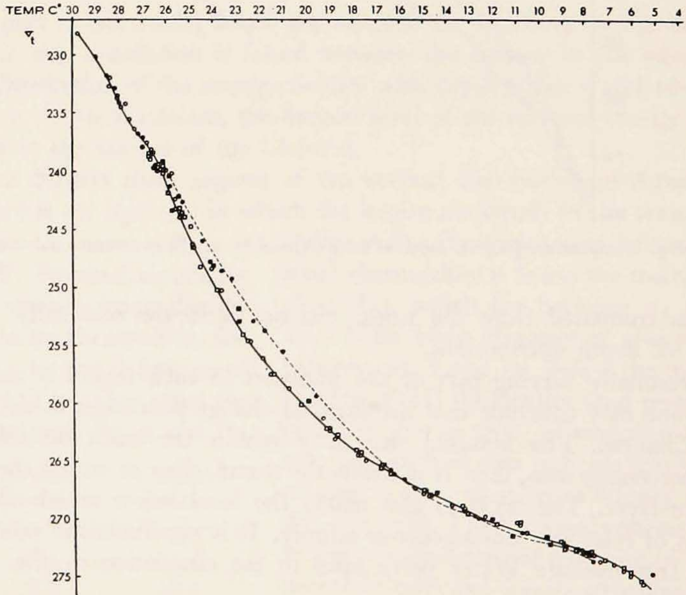

Figure 11. Temperature-density correlation for the western part of the Florida Strait: summer, solid line; winter, broken line.

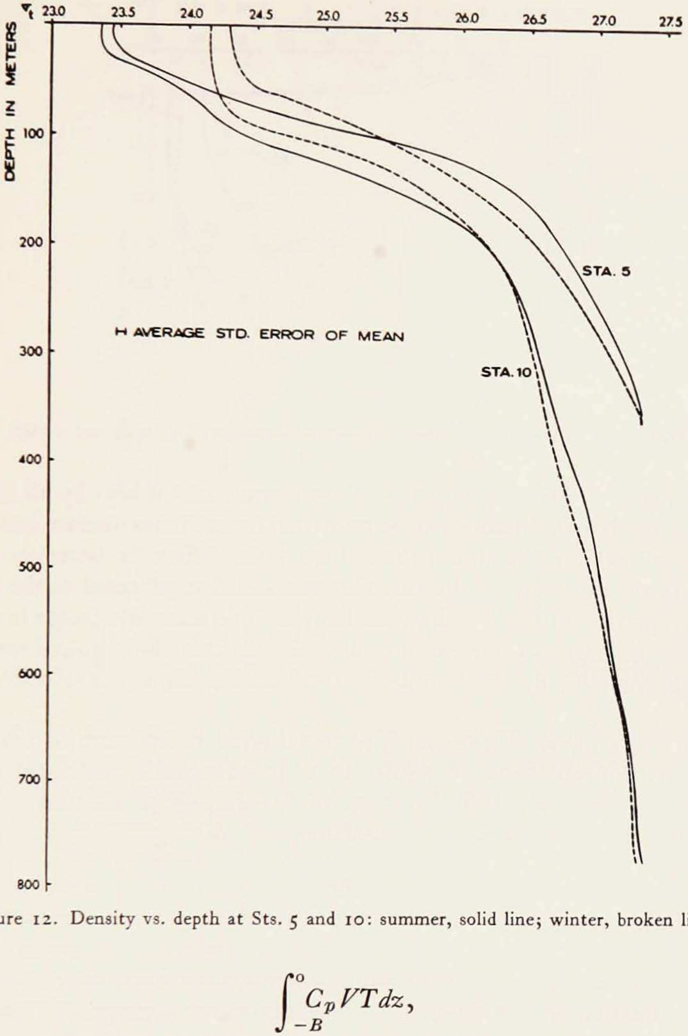

Figure 12. Density vs. depth at Sts. 5 and 10: summer, solid line; winter, broken line.

$$\int_{-B}^{0} C_p V T dz,$$

where V is the northward component of velocity and T is the temperature of the water. We recognize that this integral represents only a portion of the gross northward transport of heat and that the zero is arbitrary. However, it is adequate to define the seasonal change of heat flux through the Straits of Florida.

This integral was computed for each individual occupation of the station, and the resultant integrals were grouped according to the seasons. Fig. 14 gives the summer and winter distribution of the heat flux together with selected values of the standard deviation from the mean. The amplitude of the annual cycle of the heat transport is one-half the area between the curves and is equal to

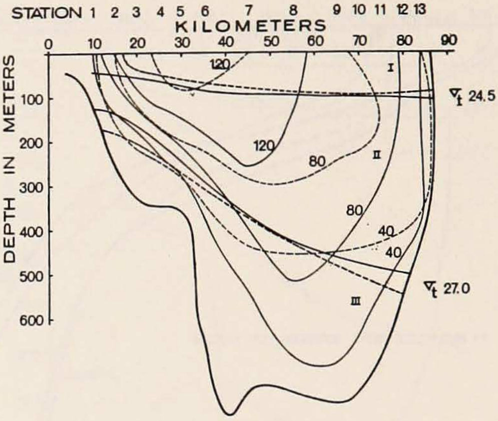

Figure 13. Relationship of velocity to density structure in summer and winter.

2.0×10^{19} cal/day. The annual net northward transport of heat by all the ocean currents in the North Atlantic can be estimated from the sea-surface heat budget to be 2×10^{19} cal/day (Malkus 1962). This is the difference between the heat advected to the north by the Florida Current and that advected to the south in the central portion of the North Atlantic gyre. The seasonal change in the heat advection is as large as the mean and does suggest that the required northward flux can be supplied by the Florida Current during the summer season.

E. THE SEA-LEVEL CHANGES. The northward component of the surface flow in the Florida Current results in a geostrophically balanced sea-level change across the Strait. If $V_S(x)$ is the surface current to the north at a location x, then the sea level across some distance L is

$$\eta_{OL} = \frac{f}{g} \int_{L_0}^{L} V_S(x)\,dx,$$

where f is the Coriolis parameter and g is the gravitational acceleration. The values of this integral for the separate crossings of the Current are compiled in Table I. Harmonic analysis for the seasonal variability yields an amplitude or 6.5 cm and a phase of 2.50 radians (the maximum value in phase with maximum transport in the early summer).

It is revealing to compare the seasonal range of the steric sea-level difference with the variability that is produced by the changing surface-current pattern. The seasonal range of the steric sea-level difference can be computed from the σ_t vs. depth given in Fig. 12. The steric sea-level height with respect to the bottom, B, is equal to

$$\int_{B}^{0} [\sigma_t - \sigma_t(B)]\,dz$$

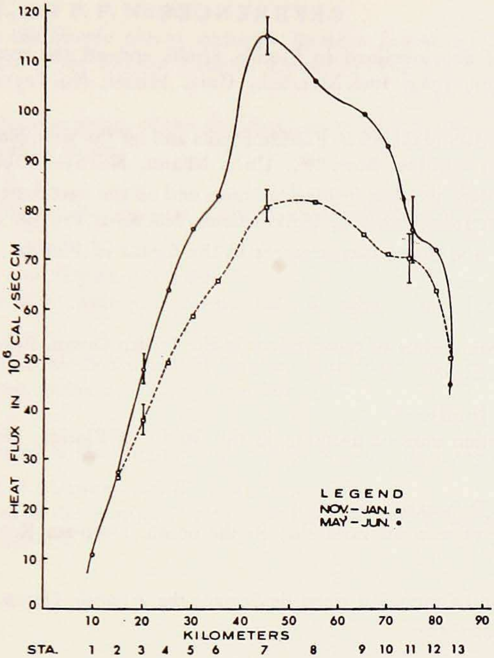

Figure 14. Heat flux through the Florida Strait in summer (solid line) and winter (broken line).

and results in the seasonal range of a sea-level difference of 2.5 cm between Sts. 5 and 10. Harmonic analysis of the geostrophically balanced sea-level difference yields a seasonal range of 12.2 cm (phase 2.5 radians) between these stations. The seasonal steric level change is principally due to the formation of the seasonal thermocline. This warm surface layer of water forms uniformly across the entire Current, and no substantial steric-level difference is found. The consequence of the observation that the steric effect is much smaller than the geostrophically balanced difference is that the seasonal changes of the pressure gradients are barotropic over the greater portion of the flow. As has been discovered before, the seasonal variability of the velocity structure penetrates to the ocean floor.

Acknowledgments. So many of our colleagues participated in the observational and computational aspects of this work that we cannot acknowledge their individual contributions; we can only thank them collectively. This program, extending over seven years, has been supported by both the National Science Foundation and the Office of Naval Research. This support is gratefully acknowledged.

REFERENCES

BROIDA, SAUL

1962. A report of data obtained in Florida Straits and off the west coast of Florida. January–June, 1962. Inst. Mar. Sci., Univ. Miami, No. 62511. 138 pp. Unpublished.

1963. A report of data obtained in Florida Straits and off the west coast of Florida. July–December, 1962. Inst. Mar. Sci., Univ. Miami, No. 63–3. 196 pp. Unpublished.

1964. A report of data obtained in Florida Straits and off the west coast of Florida. January –June, 1963. Inst. Mar. Sci., Univ. Miami, No. 64-1. 179 pp. Unpublished.

1969. Geostrophy and direct measurement in the Straits of Florida. J. mar. Res., *27*(3): 278–292.

DUING, W.

1970. The Monsoon regime of the currents in the Indian Ocean. East-west Center Press, Honolulu. 66 pp.

DUING, W., and D. JOHNSON

1972. High resolution current profiling in the Straits of Florida. Deep-sea Res., *19*(3): 259–274.

GILL, A. E., and P. P. NIILER

1973. The theory of seasonal variability in the ocean. Deep-sea Res., *20* (2): 141–177.

HELLERMAN, S.

1965. Computation of the wind stress fields over the Atlantic Ocean. Monthly Weather Rev., *93*: 239–244.

LEETMA, A.

1972. The response of the Somali Current to the southwest monsoon of 1970. Deep-sea Res., *19*(4): 319–325.

LEIPPER, D. F.

1967. A sequence of current patterns in the Gulf of Mexico. Report 67-9T, Texas A & M University. 48 pp.

LIGHTHILL, M. J.

1969. Dynamic response of the Indian Ocean to onset of southwest monsoon. Philos. Trans., *A265*: 45–92.

MALKUS, J. S.

1962. Large-scale interactions, *In*, The sea. Chap. 4: 88–294. Interscience Publishers, N.Y. 864 pp.

RICHARDSON, W. S., and W. J. SCHMITZ, JR.

1965. A technique for the direct measurement of transport with application to the Straits of Florida. J. mar. Res., *23*: 172.

RICHARDSON, W. S., and W. J. SCHMITZ, JR.

1968. On the transport of the Florida Current. Deep-sea Res., *15*: 679–693.

RICHARDSON, W. S., W. J. SCHMITZ, JR., and P. P. NIILER

1969. The velocity structure of the Florida Current from the Straits of Florida to Cape Fear. Deep-sea Res., *16*: 225–231.

SCHMITZ JR., W. J.

1969. On the dynamics of the Florida Current. J. mar. Res., *27*(1): 121–150.

SCHMITZ JR., W. J., and P. P. NIILER
1969. A note on the kinetic energy exchange between fluctuations and mean flow in the surface layer of the Florida Current. Tellus, *11*: 814–819.

STUBBS, W. O.
1971. The baroclinic structure of the Florida Current. M.S. Thesis, University of Miami, Miami, Florida. 52 pp.

THOMPSON, R. O. R. Y.
1971. Topographic Rossby waves at a site north of the Gulf Stream. Deep-sea Res., *18* (1): 1–19.

VERONIS, GEORGE, and HENRY STOMMEL
1956. The action of variable wind stresses on a stratified ocean. J. mar. Res., *15*: 43–75.

WERTHEIM, G. K.
1954. Studies of the electric potential between Key West, Florida and Havana, Cuba. Trans. Amer. geophys. Un., *35*: 872–882.

WORTHINGTON, L. V.
1959. The 18° water in the Sargasso Sea. Deep-sea Res., 5(4): 297–305.

WUNSCH, CARL, D. V. HANSEN, and B. D. ZETLER
1969. Fluctuations of the Florida Current inferred from sea level records. Deep-sea Res., *Suppl. 16*: 447–470.